

Progressive Growing of Video Tokenizers for Highly Compressed Latent Spaces

Aniruddha Mahapatra¹ Long Mai¹ Yitian Zhang^{1,2†}
David Bourgin¹ Feng Liu¹

¹Adobe Research ²Northeastern University

<https://progressive-video-tokenizer.github.io/Pro-MAG/>

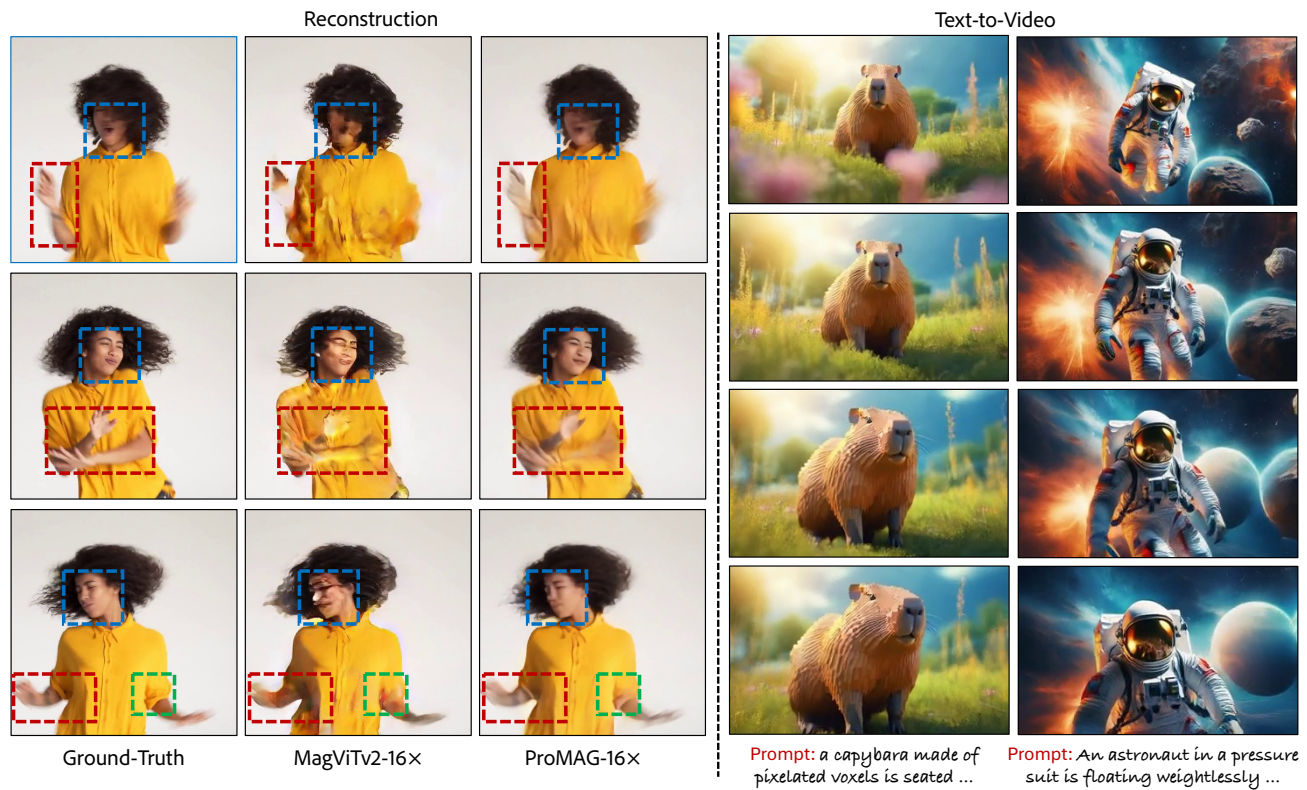


Figure 1. (left) Our video tokenizer ProMAG is capable of much more effectively reconstructing high motion videos even at very large compression ratios, like 16× temporal compression compared to baseline. Dotted boxes highlight regions where the baseline fails catastrophically. (right) We show that our highly compressed latent space (16×) is suitable for training text-to-video diffusion models.

Abstract

Video tokenizers are essential for latent video diffusion models, converting raw video data into spatiotemporally compressed latent spaces for efficient training. However, extending state-of-the-art video tokenizers to achieve a temporal compression ratio beyond 4× without increasing channel capacity poses significant challenges. In this work, we pro-

pose an alternative approach to enhance temporal compression. We find that the reconstruction quality of temporally subsampled videos from a low-compression encoder surpasses that of high-compression encoders applied to original videos. This indicates that high-compression models can leverage representations from lower-compression models. Building on this insight, we develop a bootstrapped high-temporal-compression model that progressively trains high-compression blocks atop well-trained lower-compression

[†]This work was done during an internship at Adobe Research.

models. Our method includes a cross-level feature-mixing module to retain information from the pretrained low-compression model and guide higher-compression blocks to capture the remaining details from the full video sequence. Evaluation of video benchmarks shows that our method significantly improves reconstruction quality while increasing temporal compression compared to direct extensions of existing video tokenizers. Furthermore, the resulting compact latent space effectively trains a video diffusion model for high-quality video generation with a reduced token budget.

1. Introduction

The emergence of diffusion models [15, 36] has transformed image [9, 27, 30, 32, 33] and video [4, 5, 10, 14, 16, 35, 40] generation. These models gradually transform random noise into coherent visual outputs, showcasing impressive capabilities in producing high-fidelity content [5, 8]. Latent diffusion models (LDMs)[32] have gained popularity for image and video generation[1, 33]. Unlike pixel diffusion models that operate directly on raw pixels, LDMs project pixels into a low-dimensional latent space using a variational autoencoder (VAE) [23], enabling diffusion in this reduced space. This dimensionality reduction enhances computational and memory efficiency, which is particularly crucial for video generation due to the higher dimensionality of video data compared to images.

Early latent video diffusion models (LVDMs) relied on latents extracted from each frame independently [2, 14, 35] by reusing the same VAE from image LDMs. This neglects the temporal dynamics inherent in video data, compromising the temporal consistency of the generated videos, and offers no temporal compression in the latent space. To address these limitations, the seminal work MagViT-v2 [41] pioneers a dedicated spatiotemporal video encoding that can jointly encode images and videos in the same latent space. Originally designed to encode video into discrete spatiotemporal tokens, MagViT-v2 has been widely adapted to continuous tokens for use in many state-of-the-art LVDMs [13, 24, 40, 46].

State-of-the-art video diffusion models (VDMs) utilize diffusion transformers [27] as their backbone architectures, with computational costs scaling quadratically with input token lengths. Increasing latent space compression by a factor of two in both spatial and temporal dimensions significantly enhances model efficiency. While MagViT-v2 and other video tokenizers achieve substantial spatial compression ($8\times$), their temporal compression remains limited to $4\times$. This work focuses on improving temporal compression while maintaining spatial compression at $8\times$. We found that extending MagViT-v2 by adding more temporal down/upsampling layers to boost temporal compression negatively impacts reconstruction quality. This underscores a key challenge in adapting convolutional video tokenizers for

higher compression rates: training such models from scratch necessitates simultaneous optimization of all parameters for high compression, rather than employing a hierarchical approach where different components specialize in varying levels of compression.

Interestingly, we observe that $4\times$ temporal compression MagViT-v2 can accurately reconstruct videos with $4\times$ frame subsampling (i.e., low FPS), much better than a $16\times$ temporal compression model on the original (high FPS) video. Thus, we try to answer the question: “*Can we meaningfully boost the temporal compression of video tokenizers by reusing a pretrained $4\times$ model, while keeping the number of latent channels constant?*” In this paper, we intentionally keep the latent channel dimension fixed over the progressive growing process for two reasons. First, that helps separate the effects of channel dimensions and progressive growing on the model performance. Second, one of our main goals is to achieve good latent features not only for high reconstruction quality but also for effective downstream diffusion model training. It has been observed that increasing the latent channel dimensions, while leading to a slight improvement in reconstruction, tends to make generative model training more difficult [41].

This paper makes the following main contributions:

- We adopt the continuous-token MagViT-v2 architecture as our base model and make several modifications to make it more efficient and amenable to our method of growing the model from $4\times$ to $8\times$ and $16\times$ compression. The modifications preserve the quality of the base $4\times$ MagViT-v2. We call our model **ProMAG** (abbreviation for **Progressive growing of MagViT-v2 for continuous-space tokens**).
- We present our progressive model growing technique to train ProMAG for high temporal compression ratios, achieving up to $8\times$ and even $16\times$. Notably, we are the first to achieve high-quality reconstruction with a $16\times$ temporal compression model. Evaluations on video benchmarks show that our models deliver significantly better reconstruction quality than simply extending existing video tokenizers for high compression.
- We showcase the effectiveness of our highly compressed latents for text-to-video generation with DiT. Experiments on the text-to-video evaluation benchmark [18] reveal that DiT trained with our $16\times$ temporal-compression latents achieves comparable or slightly higher quality than the standard $4\times$ compression, while significantly enhancing efficiency.

2. Related work

Latent video diffusion models. The pioneering LVDMs [2, 3, 10, 14, 26, 35] repurposed image VAEs to transform each frame of the video independently into the latent space. This caused temporal flickering in the generated video and limited the video length due to limited compression achieved by



Figure 2. **Motivation.** We highlight the key motivation of our progressive growing approach. Directly training MagViT-v2 for $16\times$ temporal compression leads to poor reconstruction quality for a 24-fps video (bottom). $s_f = 1$ stands for frame subsampling factor = 1. However, we observed that the $4\times$ temporal compression model can still accurately reconstruct a 6-fps video by feeding the same 24-fps video after subsampling frames by a factor of $4\times$, $s_f = 4$ (top). This observation implies that *it is not necessarily the large motion that leads to worse reconstruction, but that training all the weights of a much larger number of encoder and decoder blocks makes training unstable*. Since our base model ProMAG at $4\times$ temporal compression is similar to MagViT-v2, this idea is conclusion applicable for ProMAG.

image VAEs. More recent works [5, 13, 24, 40, 46] use VAEs that operate on video-level, hence mitigating both limitations of using image VAEs for video diffusion models. Building upon this, we aim to create a VAE with even higher temporal compression ($8\times$ and $16\times$) compared to the contemporary $4\times$, enabling highly efficient and longer video generation.

High compression VAEs. There have been few works recently that investigate very high compression in latent space for higher-resolution (2K or 4K) images and longer video generation. UltraPixel [31] provides an image autoencoder that can perform $24\times$ spatial compression. Concurrent work DC-AE [7] provides a solution to increase the spatial compression to as large as $128\times$ spatially. However, they have to also increase channel dimension to cope with degradation in reconstruction quality. In comparison, we only focus on increasing the temporal compression, while keeping the number of latent channels fixed to avoid making the latent space harder to learn for the diffusion model. PVDM [42] treats video as a 3D volume and encodes it into a tri-plane-like representation. CMD [43] and LaMD [17] disentangle video into content and motion components, enabling generation with image-based diffusion models. Although this enables relatively higher compression, it is not clear how to extend such factorized latent space design to fit contemporary spatiotemporal VDMs. Similarly, concurrent work MovieGen [28] achieves $8\times$ temporal compression. In comparison, our method can achieve $16\times$ temporal compression.

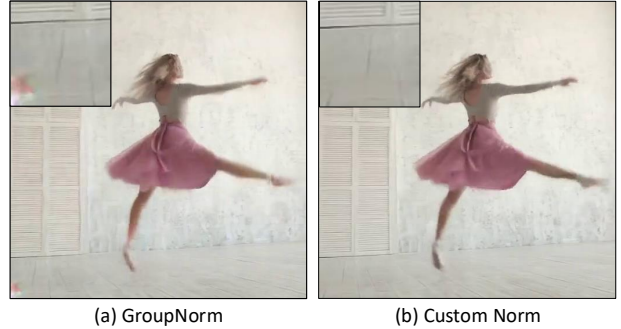


Figure 3. **‘spot artifacts’.** Our Progressive Growing approach with GroupNorm leads to the ‘spot’ like artifacts (left) at the bottom right corner in reconstructed videos. (right) Removing the mean subtraction from group normalization eliminates the spot artifacts in reconstructed frames.

Hierarchical models. Hierarchical generation has been explored most notably using generative adversarial networks (GANs) [12] to perform high-resolution image generation in stages [19, 20, 39]. These approaches first learn a generator that operates in low resolution, followed by learning additional high-resolution blocks on top in stages. Similar ideas have also been explored in image and video generation using diffusion models [1, 9, 16, 31] where content is first generated in low-resolution and then upsampled in the spatial and temporal domain using a separate model. In our work, we are inspired by ProGAN [19] and adapt the progressive learning idea to our problem of boosting the temporal compression in video tokenizers, progressively learning separate model blocks to handle different levels of compression.

3. Method

Our goal is to create a continuous-token video tokenizer with high temporal compression ratios ($8\times$ or $16\times$) and high reconstruction quality. In Section 3.1, we discuss the technical modifications we make to the MagViT-v2 implementation [41] to arrive at our (ProMAG) base model. In Section 3.2, we analyze why the base ProMAG, capable of doing $4\times$ temporal compression, has difficulties extending to $8\times$ or $16\times$ temporal compression. We discuss a method of progressively growing the ProMAG-4X model to achieve $8\times$ and consequently $16\times$ temporal compression in Section 3.2. Finally, in Section 3.3 we introduce our layer-wise spatial tiling technique during decoding to enable high-resolution encoding-decoding.

3.1. Base model: ProMAG

Following prior works [29, 40], we build our model based on the continuous-token variant of MagViT-v2 [41]. The MagViT-v2 tokenizer is composed of 3D causal convolution layers. The use of causal convolution not only enables full

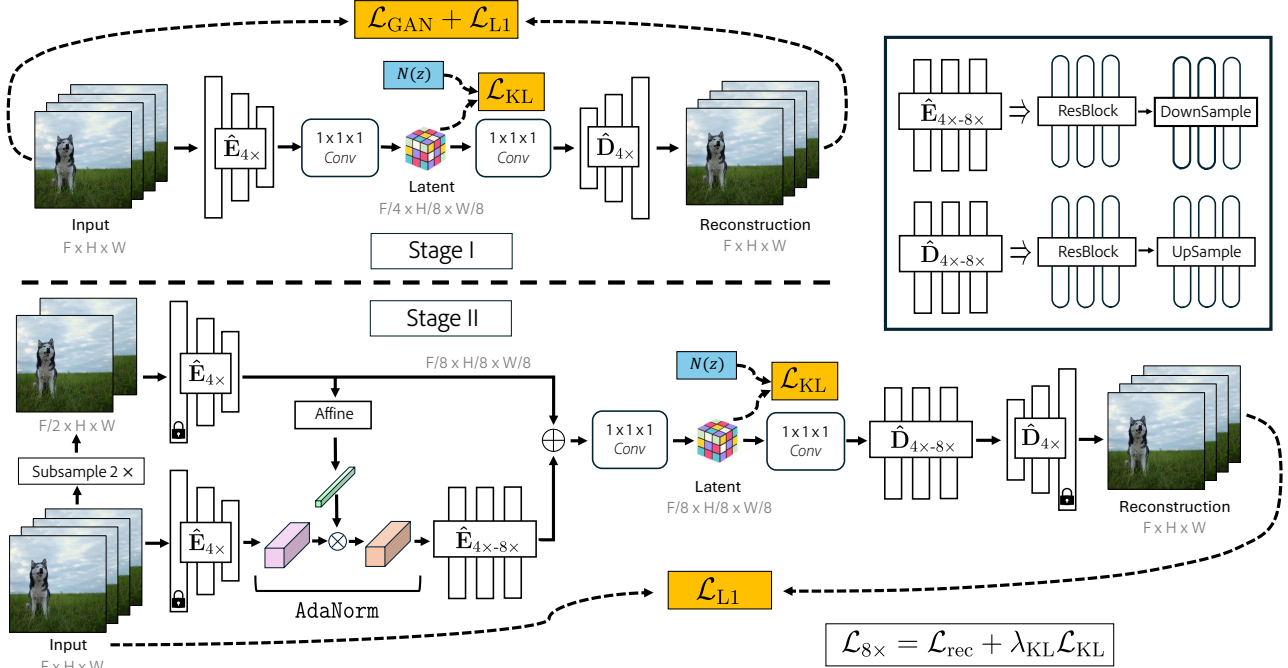


Figure 4. **Methodology.** Figure shows details of our method of progressive growing. In Stage I (top) we show a method of training our base $4\times$ video tokenizer. (bottom) we illustrate the detailed method of growing the base $4\times$ model to achieve $8\times$ temporal compression.

spatiotemporal processing but also facilitates consistent encoding of images and video data. Our model encodes an input video (or image) with $1 + k \times N$ frames into $1 + N$ latent frames, where k is the compression ratio and $N = 0$ when encoding images. MagViT-v2, by default, can perform $4\times$ temporal compression ($k = 4$) very reliably.

We make three key modifications to the base MagViT-v2 model to increase training and inference efficiency and to make it amenable to our method of progressive growing. We call our model ProMAG.

Image model initialization. Instead of training a 2D image encoder and using the weights to initialize 3D convolution kernels as in MagViT-v2 [41], we freeze the encoder of our pretrained 2D image model and use it to encode the first frame of the input video. We then train the MagViT-v2 model with 3D causal convolutions to focus only on encoding the rest of the video frames. In our experience, this makes the model training converge faster.

Efficient upsampling. MagViT-v2 encodes a 17-frame video into 5 latent frames which are decoded to 20 frames after $4\times$ temporal upsampling. The presence of three additional frames in the reconstruction is a byproduct of the fact that the first latent frame only represents a single input frame. The MagViT-v2 decoder discards these 3 reconstruction frames when generating the final output. We find this

operation to be wasteful in terms of computation and becomes a greater problem with more temporal compression. For example, in the case of $16\times$ compression on 17 frames, the decoder will output 32 frames and have to reject the first 15 frames. To mitigate this issue, in all the temporal upsampling layers of the decoder, we discard the 1^{st} frame, as it can be considered a padding frame in causal convolutions. This reduces the memory consumption significantly, especially for higher compression models, without hurting reconstruction quality.

Removing ‘spot’ artifacts. MagViT-v2 uses group normalization to normalize activations between layers. This causes ‘spot’ like artifacts when trained to progressively increase the temporal compression (Figure 3(a)). This occurs because the model tends to encode important global information in these high-norm latent pixels, as also observed in [28]. To address this phenomenon, we modify the group-normalization operation by removing the mean subtraction following [21, 22]. We found this modification effectively resolves the ‘spot’ artifacts in the reconstructed videos (Figure 3(b)).

3.2. Progressive model growing

Motivation. To increase the temporal compression of ProMAG from $4\times$ to $8\times$ or $16\times$, the standard approach is to add additional downsampling and upsampling blocks in the

bottleneck layers of the encoder and decoder respectively. In our preliminary study, we found that directly training ProMAG for $16\times$ temporal compression leads to poor reconstruction quality for a 24-fps video (Figure 2(b)). However, we observed that the $4\times$ temporal compression model can still accurately reconstruct a 6-fps video by feeding the same 24-fps video after subsampling frames by a factor of $4\times$ (Figure 2(a)). This observation implies that *it is not necessarily the large motion that leads to worse reconstruction, but that training all the weights of a much larger number of encoder and decoder blocks makes training unstable.*

Since the ProMAG- $4\times$ can accurately reconstruct a 6-fps video, our strategy is to use it as guidance for the additional bottleneck downsampling and upsampling blocks to achieve $8\times$ and $16\times$ temporal compression. This can be thought of as a guided video interpolation problem. Instead of forcing the bottleneck compression layers to learn the entire information flow, we aim to induce them to reuse the information of the $4\times$ blocks, and only learn the essential information needed to synthesize the in-between frames, which is necessary to reconstruct the full video.

Progressive model growing. Building on the above observation, we develop our progressive model growing framework for boosting the temporal compression in ProMAG. We describe in detail below our framework for growing our model from $4\times$ to $8\times$ temporal compression. Growing the model from $8\times$ to $16\times$ follows the same procedure.

Key-frame embedding. A naive way to achieve $8\times$ temporal compression using the $4\times$ model, $\mathbf{E}_{4\times}$, is to subsample the input video frames \mathbf{v} by a factor of two, ($\mathbf{v}_{//2}$), and then encode the frames with $\mathbf{E}_{4\times}$. This can be referred to as learning the key-frame encodings z_{key} , of the subsampled keyframes.

$$z_{\text{key}} = \hat{\mathbf{E}}_{4\times}(\mathbf{v}_{//2}) \quad (1)$$

where $\hat{\mathbf{E}}_{4\times}$ is the encoder blocks without the bottleneck $1 \times 1 \times 1$ layers.

Residual embedding. Now with the encodings to accurately reconstruct keyframes in the video, we only need to learn the information for the remaining frames. We denote z^* as the embedding of entire video \mathbf{v} upto the $4\times$ temporal compression blocks, $\hat{\mathbf{E}}_{4\times}$. To reach $8\times$ compression, we compress z^* through the additional $2\times$ downsampling block. However, we need to ensure that the downsampling blocks $\hat{\mathbf{E}}_{4\times-8\times}$ are aware of the information already present in z_{key} , as it only needs to preserve the remaining information to avoid redundancy. For this, we use adaptive group normalization (AdaNorm) to condition the intermediate latent, z^* , on the key-frame embeddings z_{key} before passing it to $\hat{\mathbf{E}}_{4\times-8\times}$.

$$\begin{aligned} z_{\text{inter}}^* &= \text{AdaNorm}(z_{\text{key}}, \hat{\mathbf{E}}_{4\times}(\mathbf{v})) \\ z_{\text{inter}} &= \hat{\mathbf{E}}_{4\times-8\times}(z_{\text{inter}}^*) \end{aligned} \quad (2)$$



Figure 5. **High-Resolution Reconstruction.** (left) tilting the latent before passing through the decoder leads to artifacts in the reconstructed video. (right) layer-wise tiling resolves the artifacts. The red-bordered frame at the bottom left corner represents the ground-truth frame.

We obtain the final latent z as the linear combination of both z_{key} and z_{inter} .

$$z = \text{Conv}_{1\times 1\times 1}(z_{\text{key}} + z_{\text{inter}}) \quad (3)$$

For the decoder we only add an additional bottleneck upsampling block.

Training strategy. We obtain the base $4\times$ temporal compression model by training with (1) the video-level GAN loss \mathcal{L}_{GAN} [12], (2) the L_1 reconstruction loss \mathcal{L}_{rec} , and (3) the KL-divergence loss \mathcal{L}_{KL} .

$$\mathcal{L}_{4\times} = \mathcal{L}_{\text{rec}} + \lambda_{\text{KL}}\mathcal{L}_{\text{KL}} + \lambda_{\text{GAN}}\mathcal{L}_{\text{GAN}} \quad (4)$$

We initialize the weights for the $8\times$ temporal compression model with the $4\times$ models and freeze the encoder and decoder blocks initialized from the $4\times$ model. At this stage, we only train the newly added blocks and the $1 \times 1 \times 1$ bottleneck layer using (1) the L_1 reconstruction loss \mathcal{L}_{rec} , and (2) the KL-divergence loss \mathcal{L}_{KL} . While GAN loss can slightly improve the FVD score in the reconstructed videos, it tends to introduce more visual artifacts in challenging scenarios. Therefore, we do not use it at this stage, which also makes our progressive growing process significantly more efficient.

3.3. High resolution video reconstruction

Directly using our model, ProMAG, or MagViT-v2 to encode and decode videos at high resolution (e.g. 540×960), results in out-of-memory (OOM) errors due to the VRAM-intensive 3D convolution layers.

We found the OOM issue arises only during decoding (i.e., high-resolution videos can be encoded as-is). With this in mind, we opted to encode the entire video at once and only spatially tile the encoded latent, decoding each tile separately. However, similar to tiling in RGB space, this approach results in artifacts, as seen in Figure 5 (a). In the latent tiling case, we found the issue to be a misalignment between the full, low-resolution video encoding and decoding regimen learned during training and the tiled decoding seen at inference. Specifically, we found that there

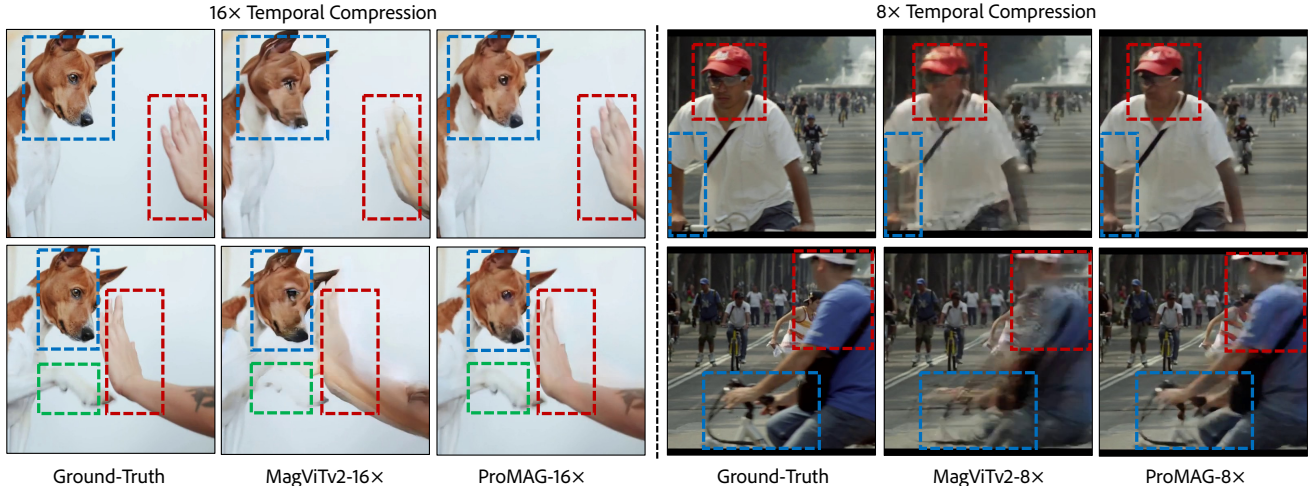


Figure 6. **Qualitative Comparison with Baseline.** Video reconstruction example for (left) 16× temporal compression, (right) 8× temporal compression. In both compression ratios, baseline MagViT-v2 causes loss of details and produces artifacts in the reconstructed frames. The dotted boxes show regions of the most difference between our results and baseline.

Method	Compression	z_dim	MCL-JCV						DAVIS					
			512×512			360×640			512×512			360×640		
			PSNR	LPIPS	rFVD	PSNR	LPIPS	rFVD	PSNR	LPIPS	rFVD	PSNR	LPIPS	rFVD
OS-VAE	8×8×4	4	30.59	11.72	120.93	29.92	12.9	168.44	27.73	15.99	405.28	26.58	17.22	424.78
OSP-VAE			30.21	11.72	120.93	29.57	8.19	122.18	27.29	10.74	298.02	26.08	11.19	327.64
CMD (p8)	8	8	23.24	17.36	1084.66	-	-	-	18.25	25.63	2097.52	-	-	-
CMD (p2)			23.50	17.36	1120.30	-	-	-	17.72	28.31	2136.59	-	-	-
MagViT-v2	8×8×4	8	30.63	6.49	58.11	30.31	6.44	57.68	28.32	7.3	129.11	26.95	7.64	151.12
ProMAG			30.99	6.53	57.91	30.37	6.53	58.14	28.43	7.38	130.56	27.07	7.67	152.07
MagViT-v2	8×8×8	8	28.47	11.17	219.36	28.33	10.73	222.09	24.02	16.7	525.1	23.82	15.55	477.19
ProMAG			30.26	8.36	96.85	29.84	8.29	108.95	26.48	11.37	360.54	25.76	11.12	337.15
MagViT-v2	8×8×16	8	26.15	14.54	255.51	25.96	14.19	265.99	21.82	20.54	728.04	21.73	19.43	695.67
ProMAG			28.31	11.2	183.4	28.27	10.74	206.3	23.89	16.9	608.43	23.71	15.74	545.87
ProMAG	8×8×4	16	32.94	4.91	34.21	32.3	4.84	39.61	30.77	4.98	93.92	29.11	5.35	83.03
MagViT-v2	8×8×8	16	28.51	10.62	135.57	29.92	7.16	84.1	27.18	8.84	243.19	26.08	9.07	260.4
ProMAG			32.06	6.94	63.64	31.61	6.27	63.59	28.7	8.32	194.79	27.55	8.39	214.47
ProMAG (w/ GAN)			31.78	6.21	53.18	31.29	6.04	59.9	28.21	7.76	160.22	27.08	7.75	197.18
MagViT-v2	8×8×16	16	28.51	10.62	135.57	28.21	10.26	141.6	24.17	14.84	427.52	23.65	14.39	393.83
ProMAG			30.02	9.24	115.25	29.83	8.72	118.17	25.64	13.89	320.8	25.21	12.99	304.21
ProMAG (w/ GAN)			29.67	8.38	99.64	29.43	7.99	99.63	25.05	12.04	274.24	24.53	11.33	289.24

Table 1. **Quantitative Comparison with Baselines on Reconstruction Quality.** Comparison with baseline methods at different compression rates and number of latent channels on MCL-JCV and DAVIS datasets. The best results are bold-faced. CMD cannot generalize to non-square aspect ratios due to its architecture. Our method achieves better reconstruction quality under all scenarios compared to baseline methods. Note: CMD with p8 and p2 are models trained with 2 different patch-sizes (according to the author’s suggestion and official repository).

was a meaningful difference in normalization statistics encountered during training and inference. To mitigate this discrepancy, we introduce a **layer-wise spatial tiling** technique: during decoding, we divide the input to *each* conv layer into overlapping spatial tiles, process each tile independently, and merge the tiles back together using linear interpolation weights to blend the overlapping components. Using this approach, we can decode into high-resolution videos without any artifacts (Figure 5 (b)).

4. Experiments

4.1. Reconstruction Quality

Implementation details. We train our models on our internal dataset of 300M images and 15M videos at 256×256 resolution. The 4×, 8×, and 16× temporal compression models are trained with 17-frame training video clips sampled at 6 fps, 12 fps, and 24 fps, respectively. Since we follow MagViT-v2’s approach of using 3D *Causal Convolution* layers for spatiotemporal processing, videos with $1 + k \times N$

frames are compressed into $1 + N$ latent frames, where k is the compression ratio. Following this, the $4\times$ models compress videos from 17 video frames to 5 latent frames, similarly, $8\times$ from 17 frames to 3, and, $16\times$ from 17 frames to 2.

Baselines. We compare our method to the following state-of-the-art methods:

- MagViT-v2 [41]. Since the official codebase is unavailable, we implement it by ourselves and train with a setting similar to our method. We also compare against two open-sourced variants, implemented in Open-SORA [46] and Open-SORA-Plan [24]. We name these baselines OS-VAE and OSP-VAE, respectively. Similar to the original MagViT-v2 implementation, both were implemented to perform $8\times$ spatial and $4\times$ temporal compression. We use the pretrained models from the official codebases.
- We also compare to CMD [43], which decomposes videos into disentangled content and motion latents. Since the weights are not publicly available, we follow the official codebase and train the models on our internal dataset.

We compare the above baselines against our base ProMAG- $4\times$ temporal compression. For more aggressive compression, $8\times$ and $16\times$, we extend and train MagViT-v2 at the target compression ratio and compare against our method.

Evaluation benchmarks. We evaluate all methods for reconstruction quality on two standard video benchmarks, MCL-JCV [38] and DAVIS 2019 (Full Resolution) [6]. Both contain 30 high-resolution videos at a 16:9 aspect ratio. We select two different settings for reconstruction, one at square crops of 512×512 , and the other after resizing the videos to 360×640 . We compare the reconstruction quality on PSNR, LPIPS [45], and Fréchet video distance (FVD) [11, 37].

Comparison on base $4\times$ compression. Before going into the realm of high compression, we evaluate all the methods on base $4\times$ temporal compression, since most of the methods, like OS-VAE [46], OSP-VAE [24], and MagViT-v2 [41] operate at this compression ratio. From Table 1, we observe that MagViT-v2 achieves better PSNR in all cases compared to both OS-VAE and OSP-VAE. Our method, ProMAG, albeit being more efficient than MagViT-v2 (Section 3.1), achieves a similar reconstruction quality for $4\times$ temporal compression.

Effectiveness of progressive growing for boosting temporal compression. We compare our method, ProMAG, against MagViT-v2 on 2 different settings, one with 8 channels and the other with 16 channels in the latent dimension for both $8\times$ and $16\times$ temporal compression. From Table 1, ProMAG, both w/ and w/o GAN training for progressive growing, achieves better reconstruction quality than MagViT-v2 directly extended to high compression. It is interesting to note that the 16-channel version of ProMAG- $8\times$ can maintain a somewhat similar reconstruction quality to ProMAG- $4\times$. Qualitative analysis in Figure 6, (left) we

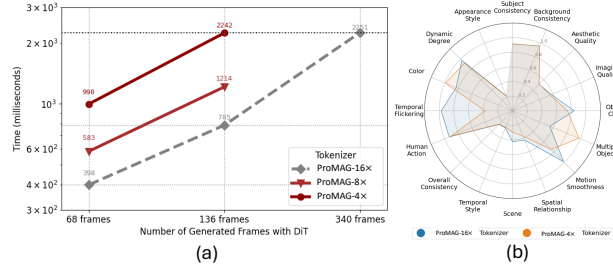


Figure 7. **Text-to-Video Evaluation.** Quantitative comparison of text-to-video generation model train on $4\times$ and $16\times$ latent space of ProMAG. (top) The graph of time taken per denoising step of the diffusion model for generating N frame video. The time is computed on H100 with Flash Attention 3 [34]. The resolution of the videos is 192×360 pixels (or 24×40 in latent dimension). We find that it takes the same time per diffusion step to generate a 136-frame video using the $4\times$ latent space, as generating a 340-frame video using the $16\times$ latent space. (bottom) Quantitative analysis different dimension on VBench [18] on generated videos with $4\times$ and $16\times$ compressed latents.

observe that at $16\times$ compression, MagViT-v2 is unable to preserve even the coarse structural details in the face or the dog or the human hand. Even at $8\times$ temporal compression, in regions of very high motion like the cyclist, MagViT-v2 blends the foreground object with the background, causing noticeable motion blur in the reconstructed videos.

4.2. T2V Quality with Compressed Latent Space

Our ultimate goal is to generate a latent space that is not only compact but more importantly, good for downstream diffusion model training. To this end, we evaluate the latent spaces produced by our models by accessing the text-to-video generation quality of the Diffusion Transformer (DiT) model trained with the resulting latent spaces. In this section, we only evaluate our $4\times$, $8\times$, and $16\times$ models and not the baseline MagViT-v2 at these compression ratios. We aim to investigate if DiT training quality and convergence degrades when trained with the highly compressed latent space of $16\times$ temporal compression compared to that trained with the original latent at $4\times$ temporal compression.

Training and implementation details. Our text-to-video diffusion model is based on the standard DiT formulation [27], composed of multiple Transformer blocks, where we replace spatial self-attention with spatial-temporal self-attention blocks. We train our model on an internal dataset of images and videos. We first train DiT on 256p images for 200K iterations, then jointly train on images and videos for about 150K more iterations.

Evaluation metrics. We evaluate the quality of text-to-video generation using VBench [18]. Following the official guidelines, we generate videos with all the 946 provided text prompts and generate videos with 5 random seeds per



Prompt: “In the aerial view of Santorini, white Cycladic buildings with blue domes are distinctively seen against ...”



Prompt: “A woman with a flower headpiece, inspired by vray tracing, features vivid colors and playful berry-punk...”

Figure 8. **Text-to-Video Generation Results.** We show very vibrant videos generated by DiT on our ProMAG-16 \times latent space. This highlights that training DiT on highly compressed latent space can still generate videos with accurate text coherence and realistic motion.

prompt. We evaluate based on all 16 quality dimensions such as ‘dynamic_degree’, ‘background_consistency’, etc.

T2V generation quality. From Figure 7(b), we find that training DiT with 16 \times temporally compressed latent space does not degrade the video generation quality on almost all dimensions compared to 4 \times compression latent. It even achieves slightly better statistics, likely due to that we can train with higher batch sizes for 16 \times temporally compressed latent due to a significantly lower number of tokens. Figure 8 shows two diverse and vibrant videos generated by DiT with 16 \times compressed latent. We find that the DiT can accurately follow the caption and generate very realistic motion.

Efficiency. Using a more compact latent space allows DiT to operate with fewer tokens, significantly reducing GPU memory and processing time. In a fixed frame length scenario (68 frames, 2.8 seconds at 24 fps), DiT with 4 \times compression generates 20 latents at 0.99s per timestep, while 8 \times compression reduces this to 12 latents at 0.58s (1.7 \times speedup). With 16 \times compression, only 8 latents are needed, achieving 0.39s per timestep (2.5 \times speedup). In a fixed token budget of 40 latent frames, the 4 \times model generates a 136-frame video (5.6s), whereas the 16 \times model produces 340 frames (14.1s), a 2.5 \times increase in video length.

5. Discussion

5.1. Progressive growing vs. progressive training

We want to investigate if the effectiveness of our method comes from our specific design towards reusing pretrained high-quality lower compression model and only learning the remaining information in the bottleneck layers, or simply just from progressive training of the model in stages by adding more bottleneck layers (w/o skip information flow).

Progressive training. In this case, we start from a pretrained 4 \times model, and then add bottleneck downsampling and up-

Method	MCL-JCV		
	PSNR	LPIPS	rFVD
MagViT-v2	28.51	10.62	135.57
ProMAG (w/o residuals & AdaNorm)	30.35	8.05	88.18
ProMAG (full method)	32.06	6.94	63.64

Table 2. **Progressive Growing v/s Progressive training.** Comparison of reconstruction quality of our full method against the naive way of progressive training on the 512x512 patches of the MCL-JCV video dataset.

sampling blocks to the encoder and decoder respectively to grow the compression rate and only train the additional blocks. This does not include the use of subsampled frames encoding or AdaNorm as our full method (Figure 4).

Evaluation. Table 2 shows the comparison of the reconstruction quality on MCL-MJC at 512x512 crops for 8 \times temporal compression. We find that progressive training (Table 2, 2nd row) by itself, improves the PSNR, LPIPS, and FVD compared to directly training MagViT-v2 from scratch for 8 \times compression. We hypothesize that it might be because with large compression and increasing channel multiples, training the video tokenizer at once may lead to difficulty in convergence. On top of that, our method of progressive growing further improves the reconstruction of all the metrics.

5.2. Progressive growing vs. frame subsampled encoding + external interpolation

The primary motivation for our method of progressive growing was that the 4 \times compression model performs very accurate reconstruction even for a 6fps video (after 4 times frame subsampling from a 24fps video).

Baseline. A very natural question would be how our method for 8 \times (or 16 \times) temporal compression would fare against the solution where we first perform 4 \times temporal compression

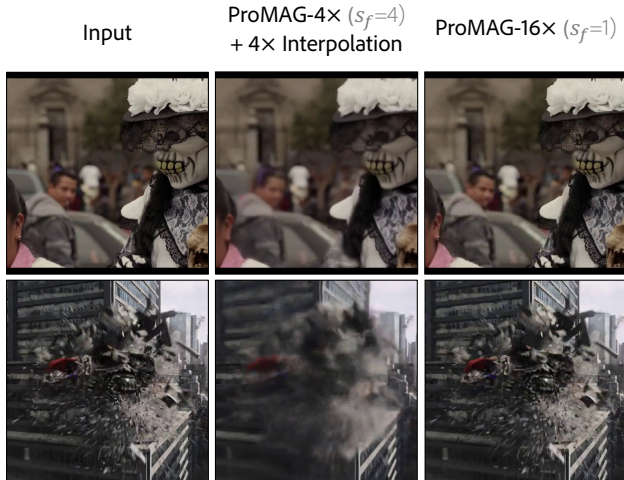


Figure 9. **Qualitative Comparison with External Interpolation.** Reconstruction comparison of our method ProMAG with $16\times$ temporal compression on a 24fps video, against a baseline where we first encode the video at low fps (with frame subsampling s_f), in this case transforming the 24fps video into 6fps with $s_f = 4$, followed by using external interpolation method to generate the 4 in-between frames. (middle) The baseline with external frame interpolation produces very blurry outputs in regions of abrupt and high-intensity motion, compared to our method ProMAG- $16\times$ operating on 24fps video directly (right). This implies in some sense, that our progressive growing approach has in some sense learned a better interpolation for reconstruction.

Method	MCL-JCV		
	PSNR	LPIPS	rFVD
ProMAG ($4\times$ w/ $s_f = 2 + 2X$ Interpolation)	30.68	8.61	230.16
ProMAG ($8\times$ w/ $s_f = 1$)	32.06	6.5	53.77
ProMAG ($4\times$ w/ $s_f = 4 + 4\times$ Interpolation)	28.42	12.35	341.14
ProMAG ($16\times$ w/ $s_f = 1$)	29.6	9.93	147.48

Table 3. **Quantitative Comparison with External Interpolation.** Reconstruction quality on MCL-JCV dataset on 512×512 crops on two different settings, one at $8\times$ and the other at $16\times$ temporal compression.

on videos subsampled with a factor of 2 (or 4), followed by using external state-of-the-art frame interpolation method like EMA-VFI [44] to perform 2X (4X) frame interpolation on the reconstructed frames. We observe, in Figure 9 that, performing external interpolation in regions of very high and complex motion causes much more blurring compared to applying our ProMAG- $16\times$ directly on the original videos.

Evaluation. From Table 3, we see that our method for $8\times$ temporal compression achieves much better reconstruction quality on PSNR, LPIPS, and FVD compared to using our $4\times$ model on subsampled frames followed by 2X interpolation. A similar trend can be observed in the case of $16\times$ temporal compression.

6. Conclusion and Limitations

In this work, we push the boundary to which we can perform temporal compression while keeping latent channel dimension constant. To this end, we propose a novel method of progressively growing our $4\times$ temporal compression video tokenizer, ProMAG, to $8\times$ and subsequently $16\times$ temporal compression. Through extensive evaluation of reconstruction and text-to-video generation, we show that (i) Our video tokenizer can perform much better reconstruction than baseline methods at very high temporal compression rates, (ii) our high compression latent space is suitable for DiT training and provides an immense boost in terms of efficiency for video generation. However, there still exists limitations, which offers opportunities for future research. In scenarios of very high and abrupt motion, our high-compression tokenizers, while perform significantly better than the directly trained baselines, also suffers from temporal artifacts in reconstruction. In addition, in DiT we find that training on increasingly more compressed latent space tends to slightly increase the time needed for convergence.

Acknowledgments. We thank Kuldeep Kulkarni, Cusuh Ham, and Gunjan Aggarwal for proofreading the paper. We are also grateful to Richard Zhang, Zhifei Zhang, Jianming Zhang, Gunjan Aggarwal, Kevin Duarte, Yang Zhou, Zhan Xu, and Lakshya for several fruitful discussions. This work was partly done while Yitian was an intern at Adobe.

References

- [1] Yogesh Balaji, Seungjun Nah, Xun Huang, Arash Vahdat, Jiaming Song, Qingsheng Zhang, Karsten Kreis, Miika Aittala, Timo Aila, Samuli Laine, et al. ediff-i: Text-to-image diffusion models with an ensemble of expert denoisers. *arXiv preprint arXiv:2211.01324*, 2022. 2, 3
- [2] Andreas Blattmann, Tim Dockhorn, Sumith Kulal, Daniel Mendelevitch, Maciej Kilian, Dominik Lorenz, Yam Levi, Zion English, Vikram Voleti, Adam Letts, et al. Stable video diffusion: Scaling latent video diffusion models to large datasets. *arXiv preprint arXiv:2311.15127*, 2023. 2
- [3] Andreas Blattmann, Robin Rombach, Huan Ling, Tim Dockhorn, Seung Wook Kim, Sanja Fidler, and Karsten Kreis. Align your latents: High-resolution video synthesis with latent diffusion models. In *Proceedings of the IEEE/CVF Conference on Computer Vision and Pattern Recognition*, pages 22563–22575, 2023. 2
- [4] Andreas Blattmann, Robin Rombach, Huan Ling, Tim Dockhorn, Seung Wook Kim, Sanja Fidler, and Karsten Kreis. Align your latents: High-resolution video synthesis with latent diffusion models. In *CVPR*, 2023. 2
- [5] Tim Brooks, Bill Peebles, Connor Holmes, Will DePue, Yufei Guo, Li Jing, David Schnurr, Joe Taylor, Troy Luhman, Eric Luhman, Clarence Ng, Ricky Wang, and Aditya Ramesh. Video generation models as world simulators. 2024. 2, 3

- [6] Sergi Caelles, Jordi Pont-Tuset, Federico Perazzi, Alberto Montes, Kevis-Kokitsi Maninis, and Luc Van Gool. The 2019 davis challenge on vos: Unsupervised multi-object segmentation. *arXiv preprint arXiv:1905.00737*, 2019. 7
- [7] Junyu Chen, Han Cai, Junsong Chen, Enze Xie, Shang Yang, Haotian Tang, Muyang Li, Yao Lu, and Song Han. Deep compression autoencoder for efficient high-resolution diffusion models. *arXiv preprint arXiv:2410.10733*, 2024. 3
- [8] Patrick Esser, Sumith Kulal, Andreas Blattmann, Rahim Entezari, Jonas Müller, Harry Saini, Yam Levi, Dominik Lorenz, Axel Sauer, Frederic Boesel, et al. Scaling rectified flow transformers for high-resolution image synthesis. In *Forty-first International Conference on Machine Learning*, 2024. 2
- [9] Oran Gafni, Adam Polyak, Oron Ashual, Shelly Sheynin, Devi Parikh, and Yaniv Taigman. Make-a-scene: Scene-based text-to-image generation with human priors. *arXiv preprint arXiv:2203.13131*, 2022. 2, 3
- [10] Songwei Ge, Seungjun Nah, Guilin Liu, Tyler Poon, Andrew Tao, Bryan Catanzaro, David Jacobs, Jia-Bin Huang, Ming-Yu Liu, and Yogesh Balaji. Preserve your own correlation: A noise prior for video diffusion models. *arXiv preprint arXiv:2305.10474*, 2023. 2, 12
- [11] Songwei Ge, Aniruddha Mahapatra, Gaurav Parmar, Jun-Yan Zhu, and Jia-Bin Huang. On the content bias in fréchet video distance. In *Proceedings of the IEEE/CVF Conference on Computer Vision and Pattern Recognition (CVPR)*, 2024. 7
- [12] Ian Goodfellow, Jean Pouget-Abadie, Mehdi Mirza, Bing Xu, David Warde-Farley, Sherjil Ozair, Aaron Courville, and Yoshua Bengio. Generative adversarial nets. In *NeurIPS*, 2014. 3, 5
- [13] Agrim Gupta, Lijun Yu, Kihyuk Sohn, Xiuye Gu, Meera Hahn, Fei-Fei Li, Irfan Essa, Lu Jiang, and José Lezama. Photorealistic video generation with diffusion models. In *European Conference on Computer Vision*, pages 393–411. Springer, 2025. 2, 3, 12
- [14] Yingqing He, Haoxin Chen, and Menghan Xia. Videocrafter: A toolkit for text-to-video generation and editing. <https://github.com/VideoCrafter/VideoCrafter>, 2023. 2
- [15] Jonathan Ho, Ajay Jain, and Pieter Abbeel. Denoising diffusion probabilistic models. In *NeurIPS*, 2020. 2
- [16] Jonathan Ho, William Chan, Chitwan Saharia, Jay Whang, Ruiqi Gao, Alexey Gritsenko, Diederik P Kingma, Ben Poole, Mohammad Norouzi, David J Fleet, et al. Imagen video: High definition video generation with diffusion models. *arXiv preprint arXiv:2210.02303*, 2022. 2, 3, 12
- [17] Yaosi Hu, Zhenzhong Chen, and Chong Luo. Lamd: Latent motion diffusion for video generation. *arXiv preprint arXiv:2304.11603*, 2023. 3
- [18] Ziqi Huang, Yanan He, Jiashuo Yu, Fan Zhang, Chenyang Si, Yuming Jiang, Yuanhan Zhang, Tianxing Wu, Qingyang Jin, Nattapol Chanpaisit, et al. Vbench: Comprehensive benchmark suite for video generative models. In *Proceedings of the IEEE/CVF Conference on Computer Vision and Pattern Recognition*, pages 21807–21818, 2024. 2, 7
- [19] Tero Karras, Timo Aila, Samuli Laine, and Jaakko Lehtinen. Progressive growing of gans for improved quality, stability, and variation. In *ICLR*, 2018. 3
- [20] Tero Karras, Samuli Laine, and Timo Aila. A style-based generator architecture for generative adversarial networks. In *CVPR*, 2019. 3
- [21] Tero Karras, Samuli Laine, Miika Aittala, Janne Hellsten, Jaakko Lehtinen, and Timo Aila. Analyzing and improving the image quality of stylegan. In *CVPR*, 2020. 4
- [22] Tero Karras, Miika Aittala, Timo Aila, and Samuli Laine. Elucidating the design space of diffusion-based generative models. *Advances in neural information processing systems*, 35:26565–26577, 2022. 4
- [23] Diederik P Kingma and Max Welling. Auto-encoding variational bayes. In *ICLR*, 2014. 2
- [24] PKU-Yuan Lab and Tuzhan AI etc. Open-sora-plan, 2024. 2, 3, 7
- [25] Jae Hyun Lim and Jong Chul Ye. Geometric gan. *arXiv preprint arXiv:1705.02894*, 2017. 12
- [26] Willi Menapace, Aliaksandr Siarohin, Ivan Skorokhodov, Ekaterina Deyneka, Tsai-Shien Chen, Anil Kag, Yuwei Fang, Aleksei Stoliar, Elisa Ricci, Jian Ren, et al. Snap video: Scaled spatiotemporal transformers for text-to-video synthesis. In *Proceedings of the IEEE/CVF Conference on Computer Vision and Pattern Recognition*, pages 7038–7048, 2024. 2
- [27] William Peebles and Saining Xie. Scalable diffusion models with transformers. In *Proceedings of the IEEE/CVF International Conference on Computer Vision*, pages 4195–4205, 2023. 2, 7, 12
- [28] Adam Polyak, Amit Zohar, Andrew Brown, Andros Tjandra, Animesh Sinha, Ann Lee, Apoorv Vyas, Bowen Shi, Chih-Yao Ma, Ching-Yao Chuang, et al. Movie gen: A cast of media foundation models. *arXiv preprint arXiv:2410.13720*, 2024. 3, 4
- [29] Can Qin, Congying Xia, Krithika Ramakrishnan, Michael Ryoo, Lifu Tu, Yihao Feng, Manli Shu, Honglu Zhou, Anas Awadalla, Jun Wang, et al. xgen-videosyn-1: High-fidelity text-to-video synthesis with compressed representations. *arXiv preprint arXiv:2408.12590*, 2024. 3
- [30] Aditya Ramesh, Prafulla Dhariwal, Alex Nichol, Casey Chu, and Mark Chen. Hierarchical text-conditional image generation with clip latents. *arXiv preprint arXiv:2204.06125*, 2022. 2
- [31] Jingjing Ren, Wenbo Li, Haoyu Chen, Renjing Pei, Bin Shao, Yong Guo, Long Peng, Fenglong Song, and Lei Zhu. Ultrapixel: Advancing ultra-high-resolution image synthesis to new peaks. *arXiv preprint arXiv:2407.02158*, 2024. 3
- [32] Robin Rombach, Andreas Blattmann, Dominik Lorenz, Patrick Esser, and Björn Ommer. High-resolution image synthesis with latent diffusion models. In *Proceedings of the IEEE/CVF Conference on Computer Vision and Pattern Recognition*, pages 10684–10695, 2022. 2, 12
- [33] Chitwan Saharia, William Chan, Saurabh Saxena, Lala Li, Jay Whang, Emily Denton, Seyed Kamyar Seyed Ghasemipour, Burcu Karagol Ayan, S Sara Mahdavi, Rapha Gontijo Lopes, et al. Photorealistic text-to-image diffusion models with deep language understanding. *arXiv preprint arXiv:2205.11487*, 2022. 2
- [34] Jay Shah, Ganesh Bikshandi, Ying Zhang, Vijay Thakkar, Pradeep Ramani, and Tri Dao. Flashattention-3: Fast and

- accurate attention with asynchrony and low-precision. *arXiv preprint arXiv:2407.08608*, 2024. 7
- [35] Uriel Singer, Adam Polyak, Thomas Hayes, Xi Yin, Jie An, Songyang Zhang, Qiyuan Hu, Harry Yang, Oron Ashual, Oran Gafni, et al. Make-a-video: Text-to-video generation without text-video data. *arXiv preprint arXiv:2209.14792*, 2022. 2, 12
- [36] Jiaming Song, Chenlin Meng, and Stefano Ermon. Denoising diffusion implicit models. In *ICLR*, 2021. 2
- [37] Thomas Unterthiner, Sjoerd Van Steenkiste, Karol Kurach, Raphael Marinier, Marcin Michalski, and Sylvain Gelly. Towards accurate generative models of video: A new metric & challenges. *arXiv preprint arXiv:1812.01717*, 2018. 7
- [38] Haiqiang Wang, Weihao Gan, Sudeng Hu, Joe Yuchieh Lin, Lina Jin, Longguang Song, Ping Wang, Ioannis Katsavounidis, Anne Aaron, and C-C Jay Kuo. Mcl-jcv: a jnd-based h. 264/avc video quality assessment dataset. In *ICIP*, 2016. 7
- [39] Ting-Chun Wang, Ming-Yu Liu, Jun-Yan Zhu, Andrew Tao, Jan Kautz, and Bryan Catanzaro. High-resolution image synthesis and semantic manipulation with conditional gans. In *CVPR*, 2018. 3
- [40] Zhuoyi Yang, Jiayan Teng, Wendi Zheng, Ming Ding, Shiyu Huang, Jiazheng Xu, Yuanming Yang, Wenyi Hong, Xiaohan Zhang, Guanyu Feng, et al. Cogvideox: Text-to-video diffusion models with an expert transformer. *arXiv preprint arXiv:2408.06072*, 2024. 2, 3, 12
- [41] Lijun Yu, José Lezama, Nitesh B Gundavarapu, Luca Versari, Kihyuk Sohn, David Minnen, Yong Cheng, Vignesh Birodkar, Agrim Gupta, Xiuye Gu, et al. Language model beats diffusion—tokenizer is key to visual generation. *arXiv preprint arXiv:2310.05737*, 2023. 2, 3, 4, 7, 12
- [42] Sihyun Yu, Kihyuk Sohn, Subin Kim, and Jinwoo Shin. Video probabilistic diffusion models in projected latent space. In *Proceedings of the IEEE/CVF conference on computer vision and pattern recognition*, pages 18456–18466, 2023. 3
- [43] Sihyun Yu, Weili Nie, De-An Huang, Boyi Li, Jinwoo Shin, and Anima Anandkumar. Efficient video diffusion models via content-frame motion-latent decomposition. *arXiv preprint arXiv:2403.14148*, 2024. 3, 7, 13
- [44] Guozhen Zhang, Yuhan Zhu, Haonan Wang, Youxin Chen, Gangshan Wu, and Limin Wang. Extracting motion and appearance via inter-frame attention for efficient video frame interpolation. In *Proceedings of the IEEE/CVF Conference on Computer Vision and Pattern Recognition*, pages 5682–5692, 2023. 9
- [45] Richard Zhang, Phillip Isola, Alexei A Efros, Eli Shechtman, and Oliver Wang. The unreasonable effectiveness of deep features as a perceptual metric. In *CVPR*, 2018. 7
- [46] Zangwei Zheng, Xiangyu Peng, Tianji Yang, Chenhui Shen, Shenggui Li, Hongxin Liu, Yukun Zhou, Tianyi Li, and Yang You. Open-sora: Democratizing efficient video production for all, 2024. 2, 3, 7

A. Progressive Growing - from 8× to 16× Temporal Compression

In Figure 2 we illustrate our method of growing the temporal compression of the 4× video tokenizer to 8× temporal compression. In Figure 11, we show the details of our entire method, i.e., growing the base 4× model to 8× then ultimately to 16× temporal compression in 3 stages. Note that all the parameter weights in the subsequent are initialized from their corresponding parameters in the previous stage. The newly added parameters are initialized with random weights.

B. ProMAG Implementation Details

Model Architecture. In Table 4, we describe the details of our tokenizer architecture for 4×, 8× and 16× temporal compression models. The encoder and decoder design of our model, ProMAG follows MagViT-v2 structure. The discriminator is taken from Stable Diffusion VAE [32], where we replace the Conv2D with Conv3D.

Training Hyperparameters. We provide additional detailed training hyper-parameters for our models as listed below:

- Video input: 17 frames, frame stride 1, 256 × 256 resolution.
- Reconstruction loss weight: 1.0.
- Generator loss type: Hinge Loss [25].
- Generator adversarial loss weight: 0.1 for 4× and 0.0 for 8× and 16× (Note: we do not use discriminator to progressively grow the model to 8× and 16× temporal compression.)
- Discriminator gradient penalty: 0.0 r1 weight.
- VGG Perceptual loss weight: 1.0.
- KL-Divergence loss weight: 1e-12.
- Tokenizer Learning rate: 0.0001.
- Tokenizer Optimizer Params: Adam with $\beta_1 = 0.9$ and $\beta_2 = 0.99$.
- Tokenizer weight decay: 0.0001
- Discriminator Learning rate: 0.0001.
- Discriminator Optimizer Params: Adam with $\beta_1 = 0.9$ and $\beta_2 = 0.99$.
- Discriminator weight decay: 0.0001
- Training iterations: 300K for 4× model, 100K for 8× model (on top of 4× model), 100K for 16× model (on top of 8× model).
- Global Batch size: 32.

C. Text-to-Video Implementation Details

Model Architecture. Our text-to-video the diffusion model is based on the standard DiT [27], composed of multiple Transformer blocks, where we replace spatial self-attention with spatial-temporal self-attention blocks. The model architecture is similar to the diffusion transformer in

CogVideoX [40]. Following them, we also keep the number of model parameters to be around 5B.

Dataset Details. We train on our internal dataset of 300M images and 1M videos. Images contain different aspect ratios, while videos are of 192x360 resolution. We train using a relatively small scale and low resolution since the computation cost for training text-to-video models is very enormous. Additionally, our main focus in training the text-to-video model is to verify that our extremely compressed latent space (16× temporal compression) is compatible with DiT training and can achieve a similar quality to 4× compressed latent space. Our goal is not to compete with state-of-the-art text-to-video models.

Training Details. Following standard practices [10, 13, 16, 35], we train our text-to-video diffusion model in 2 stages. In the first stage (image pertaining), we train the model only on images. In the second stage (joint training), we train the model jointly on both images and videos. We train the first stage for about 200K iterations and the second stage for around 150K additional iterations. We train our models on 8 nodes of H100 (64 GPUs in total).

Training on Longer Videos. In Section 4.2, we discuss that due to the highly compact nature of our 16× latent space, we can use the same token budget for 340 frames (= 20 latent frames for 16× temporal compression), which is the same as 136 frames with 4× temporal compression. To verify the generation quality of very long videos 340 frames (or 14.1s) video at 24fps, we also train a text-to-video model for this. More specifically, we only finetune our text-to-video model trained on 16× temporally compressed latent space for an additional 10K iterations on video training of 340 frames.

D. Resolving Jump Issues: Overlapping Frame Reconstruction and T2V

Following MagViT-v2 [41], train ProMAG on 17 frame video, for all 4×, 8× and 16× temporal compression ratio. We found that since we train the model on 17 frames, we can only do encoding and decoding with 17 (or fewer) frames. We found a similar case is true with MagViT-v2. We found that reconstruction of more than 17 frames causes deterioration in the reconstruction results beyond 17 frames, like blurring, or in some cases checkerboard-like artifacts. Thus, for reconstruction (or text-to-video generation), we need to process it in chunks of 17 frames at a time for an N-frame video. This causes a jump-like effect in regions of high-frequency details every 17 frames. This jump is much less noticeable in reconstruction results, but more noticeable in the text-to-video generation results. For video generation, this jumping effect reduces with more training iterations but persists slightly. To counteract this, we perform encoding in chunks with an overlap of a few frames (in this case of 4 frames) Figure 10. The overlapping regions in the output are blended in pixel space with linear interpolated weights. This

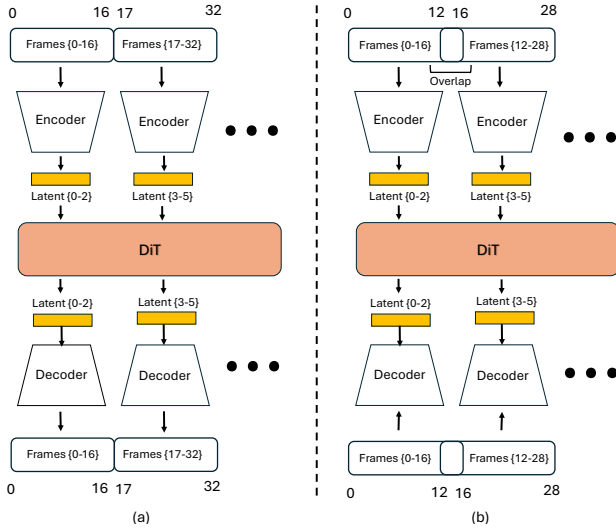


Figure 10. **Text-to-Video with overlapping frames.** (left) The conventional way of generating videos, where frames are encoded into overlapping chunks. This results in jumps like artifacts across chunks in the generated video in regions of high frequency details. (right) Generating video with chunks with overlap (here of 4 frames). The overlapped regions in the output is blended in pixel-space with linear interpolated weights. This resolves the jumping artifacts.

resolves the jumping artifacts perceptually in reconstruction and video generation results.

E. CMD [43] Baseline Implementation Details.

Since the model weights for CMD [43] are not available in their official repository, we use the provided implementation and train with the originally provided settings to train on our internal data. We train on 256×256 resolution videos (because it was the maximum we could fit on A100 GPUs). We use a batch size of 1 per GPU but use 32 A100 GPUs to accommodate the recommended batch size by the authors for training. We also contacted the authors of CMD [43] for recommendations. The author recommended we also experiment with using the patch size of 8 ($p=8$) for potentially better efficiency and quality. Thus we provide results for both the settings in Table 1. We evaluate on a resolution of 512×512 . CMD transforms a video of 8 frames of 512×512 into a content code z_c of dimension $3 \times 512 \times 512$ and a motion code z_m of dimension $8 \times 8 \times 512$. We found that CMD could only operate on square patches and not on a resolution of 360×640 .

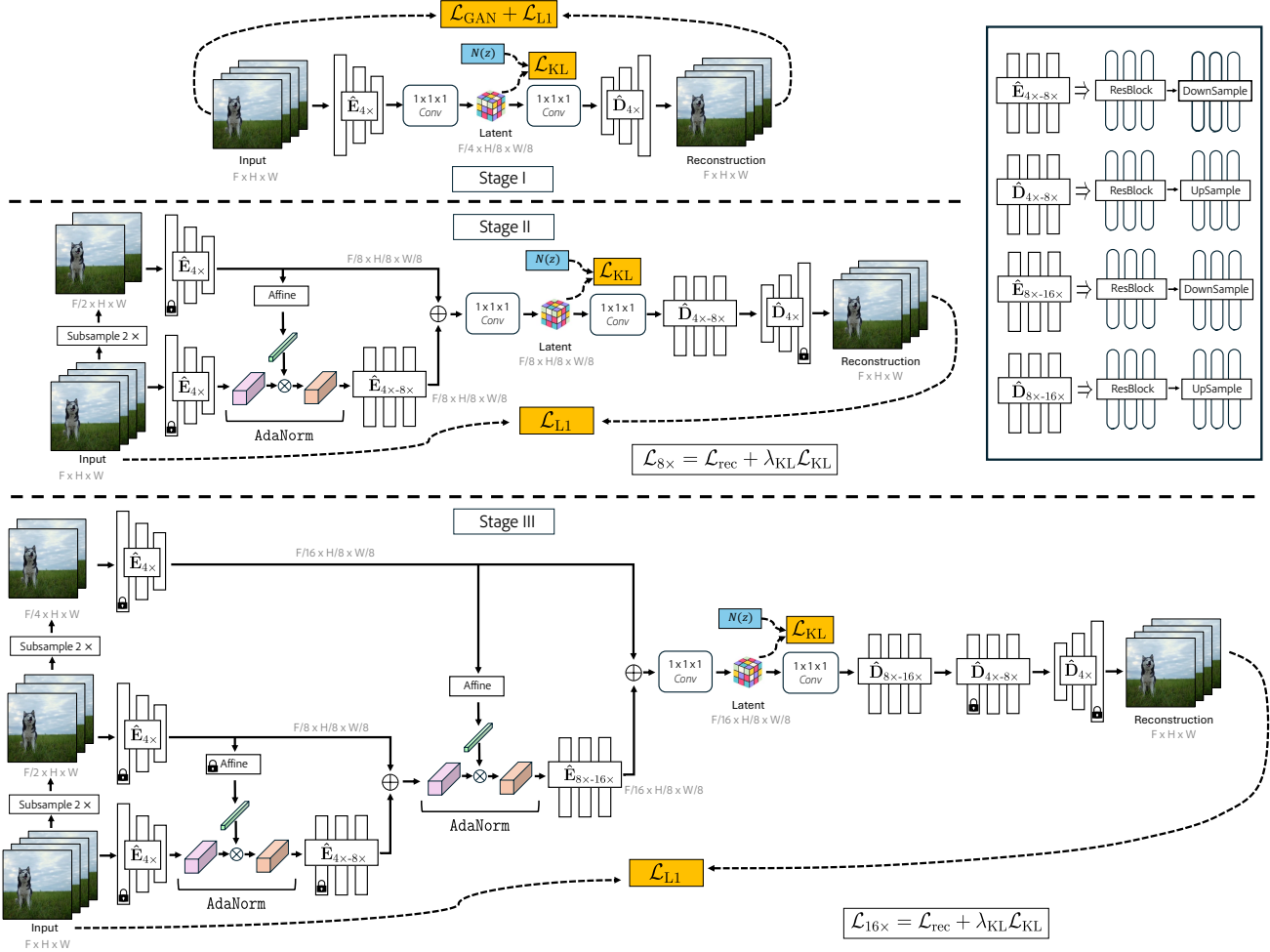


Figure 11. **Methodology.** Figure shows details of our complete method of progressive growing for extending the temporal compression to 16× from 4× compression. In Stage I (top) we show a method of training our base 4× video tokenizer. (middle) Stage II we illustrate the detailed method of growing the base 4× model to achieve 8× temporal compression. (bottom) Stage III we extend the 8× temporal compression model to achieve 16× temporal compression. $\mathcal{N}(z)$ represent a standard normal distribution.

Encoder Config	4×	8×	16×
inputs	pixels	pixels	pixels
input size	$17 \times 256 \times 256$	$17 \times 256 \times 256$	$17 \times 256 \times 256$
video fps	6	12	24
latent dimension	$5 \times 32 \times 32$	$3 \times 32 \times 32$	$2 \times 32 \times 32$
Conv-type	CausalConv3D	CausalConv3D	CausalConv3D
base channels	128	128	128
channel multipliers	1,2,4,6	1,2,4,6,6	1,2,4,6,6,6
spatial downsampling strategy	true,true,true,false	true,true,true,false,false	true,true,true,false,false,false
temporal downsampling strategy	false,false,true,true	false,false,true,true,true	false,false,true,true,true,true
downsampling strategy	strided Conv	strided Conv	strided Conv
number of residual blocks	2	2	2
z_channels	256	256	256
z_dim (number of channels in latent)	8 (or 16)	8 (or 16)	8 (or 16)
Decoder Config			
outputs	pixels	pixels	pixels
input (latent) dimension	$5 \times 32 \times 32$	$3 \times 32 \times 32$	$2 \times 32 \times 32$
output size	$17 \times 256 \times 256$	$17 \times 256 \times 256$	$17 \times 256 \times 256$
Conv-type	CausalConv3D	CausalConv3D	CausalConv3D
base channels	128	128	128
channel multipliers	6,4,2,1	6,6,4,2,1	6,6,6,4,2,1
spatial downsampling strategy	true,true,true,false	false,true,true,true,false	false,false,true,true,true,false
temporal downsampling strategy	false,true,true,false	true,false,true,true,false	true,true,false,true,true,false
downsampling strategy	nearest + Conv	nearest + Conv	nearest + Conv
number of residual blocks	3	3	3
z_channels	256	256	256
Discriminator Config			
discriminator type	patchGAN		
inputs	pixels		
input size	$17 \times 256 \times 256$		
number of layers	3	None	None
kernel size	$3 \times 4 \times 4$		
base channels	64		
Conv-type	Conv3D		

Table 4. Details of the encoder and decoder configurations of our video tokenizer ProMAG, and the discriminator configuration for different temporal compression ratios 4×, 8× and 16×. We use discriminator only for training the 4× base model.